

# $\Xi$ Hyperon Photoproduction from Threshold to 5.4 GeV with the CEBAF Large Acceptance Spectrometer

---

PhD Defense Presentation

John Theodore Goetz

B.M.K. Nefkens, Committee Chair  
UCLA Dept. Physics & Astronomy

November 1, 2010

UCLA

Jefferson Lab  
Thomas Jefferson National Accelerator Facility

# Outline of Part I: Cascade Hyperons and g12

- 1 Motivation
  - The Strong Force
  - Cascades ( $\Xi$ )
  - Photoproduction of  $\Xi$ 's
- 2 The g12 Experiment
  - The CLAS Detector
  - g12 Data and Reconstruction
- 3 g12 Kaon Data
  - Missing Mass Technique
  - Missing Mass off  $K^+K^+$
  - Sources of Background

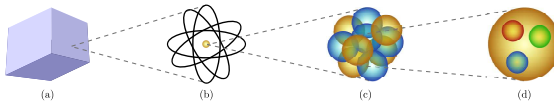
# Outline of Part II: Results From g12

- 4  $\Xi$  Excitation Functions
  - Calculation Technique
  - Simulations and Acceptance
  - $\Xi$  Yields and Excitation Functions
- 5 Search for Higher Mass  $\Xi^*$ 
  - Upper Limit Calculation Technique
  - Upper Limits
- 6 Search for Iso-Exotics
  - Estimated Sensitivity
  - $\Xi$  Iso-Exotics
  - $\Sigma$  Iso-Exotics
- 7 Conclusions
  - Summary
  - Future Work
  - Specific Issue: g6c plot

## Part I

# Cascade Hyperons and the g12 Experiment

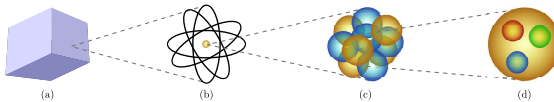
# The Forces of Nature



Four known forces: gravitational, electromagnetic, weak, strong

- The gravitational force is always attractive
- The electromagnetic force can be attractive or repulsive
- The weak force is responsible for neutrino interaction
- The strong force is either attractive or repulsive depending on the range of the particles (quarks)

# The Forces of Nature



Four known forces: gravitational, electromagnetic, weak, strong

- The gravitational force is always attractive
- The electromagnetic force can be attractive or repulsive
- The weak force is responsible for neutrino interaction
- The strong force is either attractive or repulsive depending on the range of the particles (quarks)

To complicate matters, the particles that interact via the strong force are only found in specific combinations and are never isolated

# Baryons and the Cascades

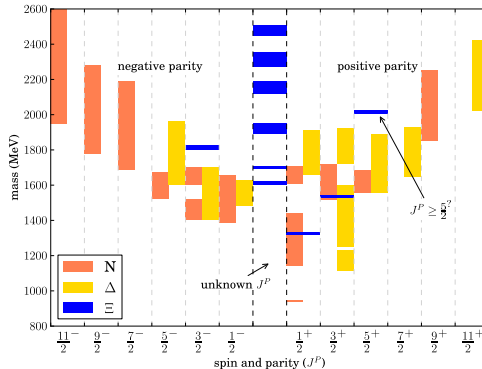
Quarks $\text{spin} = 1/2$		
Flavor	Approx. Mass $\text{GeV}/c^2$	Electric charge
<b>u</b> up	0.003	2/3
<b>d</b> down	0.006	-1/3
<b>c</b> charm	1.3	2/3
<b>s</b> strange	0.1	-1/3
<b>t</b> top	175	2/3
<b>b</b> bottom	4.3	-1/3

- The strong force is what binds the three quarks inside the proton
- There are six flavors of quarks
- This study involves only the lightest three

$\Xi$  States are identified by the quantum numbers:

- $Baryon = 1$
- $Strangeness = -2$
- $Q \in \{-1, 0\}$

# Baryons and the Cascades



In order to study the strong interaction, we look at  $qqq$  systems with two strange quarks. They are narrow and SU(3) symmetry suggests a 1:1 correspondence between the Xi spectrum and N/ $\Delta$ 's

## Previous Investigations

virtually all evidence for  $\Xi^*$  states come from measuring the decay particles directly in hadron-production experiments such as:

- $K^- p \rightarrow \Xi^- K^+$
- $\Sigma^- p \rightarrow \Xi^0 p K^+$

photoproduction provides another way to measure the cascades:

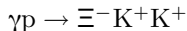


## Previous Investigations

virtually all evidence for  $\Xi^*$  states come from measuring the decay particles directly in hadron-production experiments such as:

- $K^- p \rightarrow \Xi^- K^+$
- $\Sigma^- p \rightarrow \Xi^0 p K^+$

photoproduction provides another way to measure the cascades:

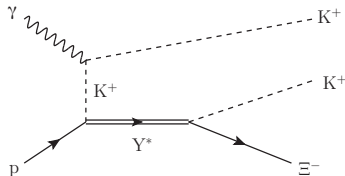


# Photoproduction of $\Xi$ 's

Allows the cascade to be identified by the photon and two  $K^+$ 's

There are a few requirements to this avenue of investigation

- photon (beam) energy measurement
- four-momenta of the two  $K^+$ 's
- sufficient acceptance for the kaons
- understanding of sources of background



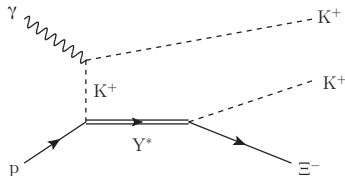
The CLAS detector at JLab satisfies these requirements

# Photoproduction of $\Xi$ 's

Allows the cascade to be identified by the photon and two  $K^+$ 's

There are a few requirements to this avenue of investigation

- photon (beam) energy measurement
- four-momenta of the two  $K^+$ 's
- sufficient acceptance for the kaons
- understanding of sources of background



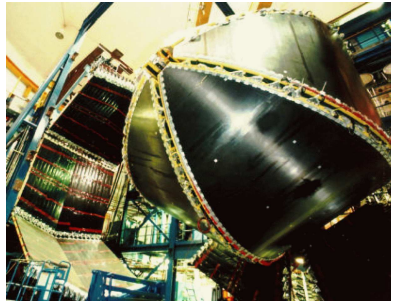
The CLAS detector at JLab satisfies these requirements

# The CLAS Detector

JLab from the air



The CLAS Detector (upstream)





# g12 Acquired Statistics

Commissioning and Data taken over 70 calendar days  
April 1<sup>th</sup> – June 9<sup>th</sup>, 2008

## Production Data

44.2 days active DAQ  
~63% of calendar time  
Beam Current: 65 nA  
DAQ rate ~8 kHz  
26.2 G triggers (events)

Size of Raw Data: 126 TB

Reconstruction Expands this by a  
factor of 2.5

"cooked" data > 300 TB

# g12 Acquired Statistics

Commissioning and Data taken over 70 calendar days  
April 1<sup>th</sup> – June 9<sup>th</sup>, 2008

## Production Data

44.2 days active DAQ  
~63% of calendar time  
Beam Current: 65 nA  
DAQ rate ~8 kHz  
26.2 G triggers (events)

Size of Raw Data: 126 TB

Reconstruction Expands this by a  
factor of 2.5

“cooked” data > 300 TB

# Calibration and Reconstruction

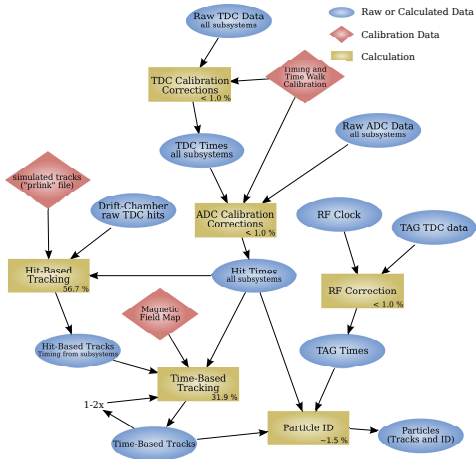
## Primary Calibrators

- C. Bookwalter, FSU (TOF)
- P. Eugenio, PhD., FSU (coord)
- **J. Goetz, UCLA (recons.)**
- L. Guo, PhD., FIU (coord)
- V. Kubarovsky, PhD., JLab (coord)
- M. Paolone, PhD., USC (EC, CC)
- **J. Price, PhD., CSUDH (coord)**
- M. Saini, FSU (RF, ST, TAG)
- D. Schott, FIU (DC)
- B. Stokes, PhD., GWU (DC)
- A. Vlassov, PhD., JLab (CC)
- D. Weygand, PhD., JLab (coord)
- M. Wood, PhD., Canisius (EC)

Calibration of the g12 data took this team a year and three months.

- My specific role was to ensure the reconstruction of tracks (four-vectors) from the raw data was done correctly and efficiently
- This involved debugging several programs which were developed over two decades by approx. two dozen people using a mix of FORTRAN, C, C++, and various scripting languages

# Reconstruction - Algorithm

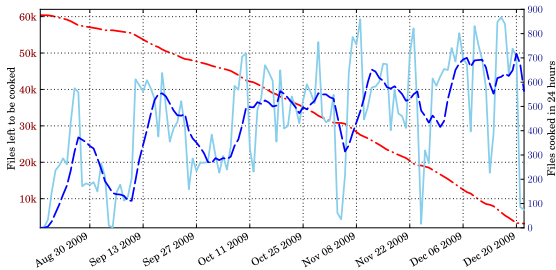


I developed this flowchart of the reconstruction algorithm and the corresponding expansions for tracking in the dissertation

There have been other studies of the reconstruction algorithm used by CLAS, but this is the first I know of that obtained the relative processing time for each step.

# Reconstruction - Timeline

The reconstruction of raw data to an analysis-ready “cooked” version took four months using the computing farm at JLab.



- Sept: higher priority
- Oct: increased cache
- Nov & Dec: more CPUs

# Analysis Framework

The single-kaon skim we initially made on the data consisted of 30% of the cooked data (about 100 TB)

This made it very difficult to read through quickly.

I developed my own variably-sized ntuple using the Serialization library from the BOOST project in C++

- this effectively converted the cooked data to zipped ASCII files
- resulting single kaon data (from 90 TB) was 1.6 TB

The 1.6 TB can be analyzed in about 1.5 days using our own farm (next door)

# Analysis Framework

The single-kaon skim we initially made on the data consisted of 30% of the cooked data (about 100 TB)

This made it very difficult to read through quickly.

I developed my own variably-sized ntuple using the Serialization library from the BOOST project in C++

- this effectively converted the cooked data to zipped ASCII files
- resulting single kaon data (from 90 TB) was 1.6 TB

The 1.6 TB can be analyzed in about 1.5 days using our own farm (next door)

# Analysis Framework

The single-kaon skim we initially made on the data consisted of 30% of the cooked data (about 100 TB)

This made it very difficult to read through quickly.

I developed my own variably-sized ntuple using the Serialization library from the BOOST project in C++

- this effectively converted the cooked data to zipped ASCII files
- resulting single kaon data (from 90 TB) was 1.6 TB

From this ntuple, I produced all the original histograms shown in the dissertation. Some images were produced with ROOT and others with the Scientific Python (SciPy) and “Matplotlib” packages.

# Missing Mass Technique

$$\gamma p \rightarrow K^+ K^+ X^-$$

- since we wish to use the missing mass technique, we must first determine its accuracy by looking at known states.
- For kaon data, we will start with singly strange baryons ( $\Sigma$ 's and  $\Lambda$ 's)
- Note that these data were calibrated mostly with exclusive pion events:  $\gamma p \rightarrow p\pi^+\pi^-$

# Missing Mass Technique

$$\gamma p \rightarrow K^+ K^+ X^-$$

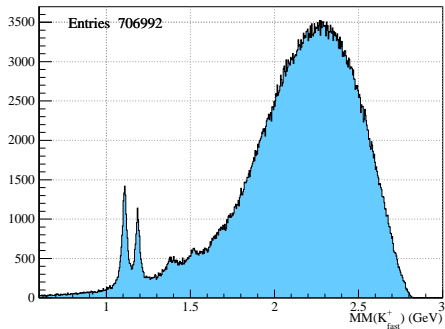
- since we wish to use the missing mass technique, we must first determine its accuracy by looking at known states.
- For kaon data, we will start with singly strange baryons ( $\Sigma$ 's and  $\Lambda$ 's)
- Note that these data were calibrated mostly with exclusive pion events:  $\gamma p \rightarrow p \pi^+ \pi^-$

# MM( $K^+$ )

$$\gamma p \rightarrow K^+ X^0$$

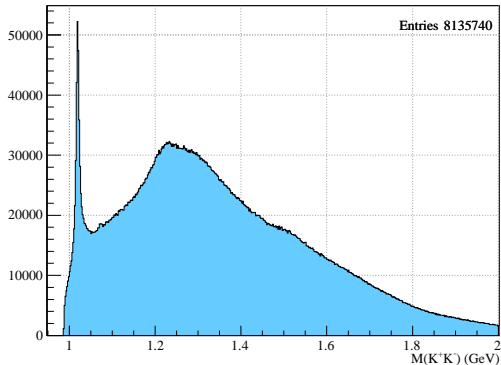
## Measured Masses (MeV)

- $\Lambda = 1109.4 \pm 0.25$   
PDG = 1116
- $\Sigma^0 = 1186.6 \pm 0.4$   
PDG = 1192
- $\Sigma^{*0} = 1385 \pm 7$   
PDG = 1384  
PDG:  $\Lambda^*(1405)$
- $\Lambda^* = 1518 \pm 3$   
PDG = 1520



# $M(K^+K^-)$

$$\gamma p \rightarrow \varphi X^+ \\ (\varphi \rightarrow K^+K^-)$$

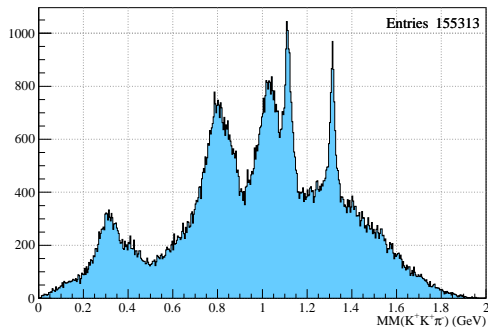


- $\varphi = 1019.5 \pm 0.2$   
PDG = 1019

# MM( $K^+K^+\pi^-$ )

$$\gamma p \rightarrow K^+K^+\pi^- \chi^0$$

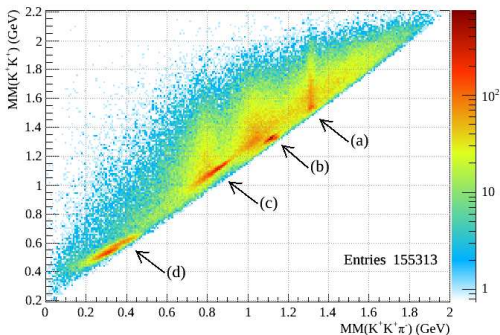
- $\Lambda = 1113.2 \pm 0.5$   
PDG = 1116
- $\Xi^0 = 1313.8 \pm 0.4$   
PDG = 1315
- secondary peaks from misidentified pions and where the  $\pi^-$  is associated with the decay of the  $\chi^0$



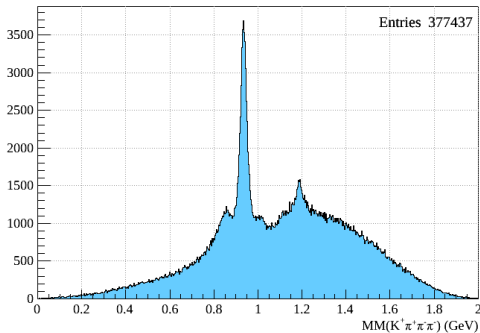
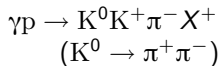
# MM( $K^+K^+\pi^-$ )

$$\gamma p \rightarrow K^+K^+\pi^- X^0$$

- $\Lambda = 1113.2 \pm 0.5$   
PDG = 1116
- $\Xi^0 = 1313.8 \pm 0.4$   
PDG = 1315
- secondary peaks from misidentified pions and where the  $\pi^-$  is associated with the decay of the  $X^0$



# MM( $K^+\pi^+\pi^-\pi^-$ )

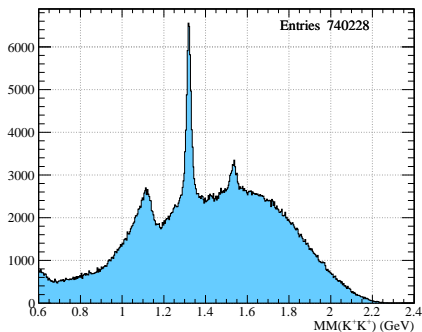


- $p = 937 \pm 1$   
PDG = 938
- $\Sigma^+ = 1186.8 \pm 1.8$   
PDG = 1189
- secondary peaks will be revisited in the search of iso-exotics

# MM( $K^+K^+$ )

$$\gamma p \rightarrow K^+K^+X^-$$

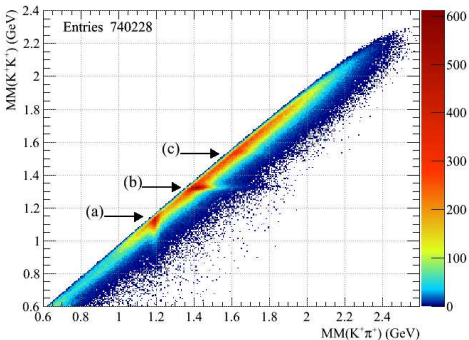
- basic timing and vertex selections only
- $\Xi^- = 1320.2 \pm 0.2$  MeV  
PDG =  $1321.71 \pm 0.07$
- $\Xi^{*-} = 1535.2 \pm 0.8$  MeV  
PDG =  $1535.0 \pm 0.6$
- misidentified pion events show up as vertical bands



# MM( $K^+K^+$ )

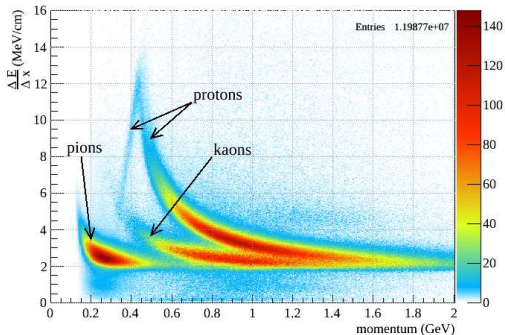
$$\gamma p \rightarrow K^+K^+X^-$$

- basic timing and vertex selections only
- $\Xi^- = 1320.2 \pm 0.2$  MeV  
PDG =  $1321.71 \pm 0.07$
- $\Xi^{*-} = 1535.2 \pm 0.8$  MeV  
PDG =  $1535.0 \pm 0.6$
- misidentified pion events show up as vertical bands



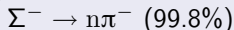
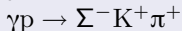
# TOF Energy Deposit Cut

- kaons identified from  $\phi(1020)$  and  $\Xi^-(1320)$  signals
- number of kaons, pions and protons were normalized in this to bring out the kaon band
- this cut was used as a consistency check of the particle ID which was based on timing



# Proton Cut

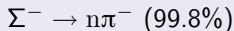
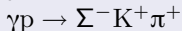
- proton can be used to remove the  $\Sigma^-(1189)$  events:



- affects  $\Sigma^{*-}$  events differently from  $\Xi^{*-}$  events  
since the  $\Xi^{*-}$ 's are more likely to decay to a proton
- Because the reductions in the  $\Xi$  signals and the  $\Sigma^{*-}$  background are different, this is a direct test of the measurements of the events in the peaks

# Proton Cut

- proton can be used to remove the  $\Sigma^-(1189)$  events:



- affects  $\Sigma^{*-}$  events differently from  $\Xi^{*-}$  events

since the  $\Xi^{*-}$ 's are more likely to decay to a proton

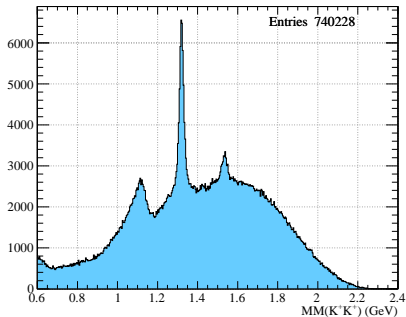
- Because the reductions in the  $\Xi$  signals and the  $\Sigma^{*-}$  background are different, this is a direct test of the measurements of the events in the peaks

# Proton Cut

- proton can be used to remove the  $\Sigma^-(1189)$  events:  
 $\gamma p \rightarrow \Sigma^- K^+ \pi^+$   
 $\Sigma^- \rightarrow n \pi^-$  (99.8%)
- affects  $\Sigma^{*-}$  events differently from  $\Xi^{*-}$  events  
since the  $\Xi^{*-}$ 's are more likely to decay to a proton
- Because the reductions in the  $\Xi$  signals and the  $\Sigma^{*-}$  background are different, this is a direct test of the measurements of the events in the peaks

# Primary Event Selections

$$\gamma p \rightarrow K^+ K^+ X^-$$



## Event Selections

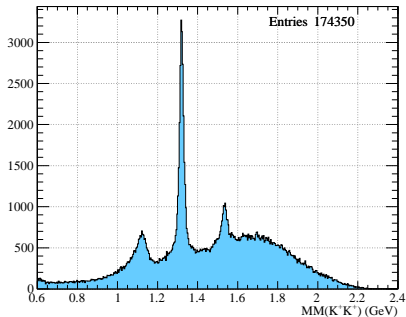
- Basic Timing Cuts
- TOF Energy Dep.
- Proton

$$\Xi^- (1320): 22690 \pm 250$$

$$\Xi^- (1530): 4330 \pm 240$$

# Primary Event Selections

$$\gamma p \rightarrow K^+ K^+ X^-$$



## Event Selections

- Basic Timing Cuts
- TOF Energy Dep.
- Proton

$\Xi^-$  (1320):  $15190 \pm 150$

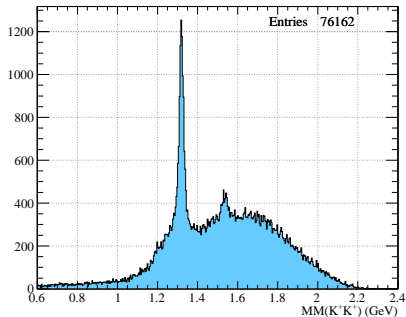
67% of basic cuts

$\Xi^-$  (1530):  $3020 \pm 120$

70% of basic cuts

# Primary Event Selections

$$\gamma p \rightarrow K^+K^+X^-$$



## Event Selections

- Basic Timing Cuts
- TOF Energy Dep.
- Proton

$\Xi^-$  (1320):  $7557 \pm 125$

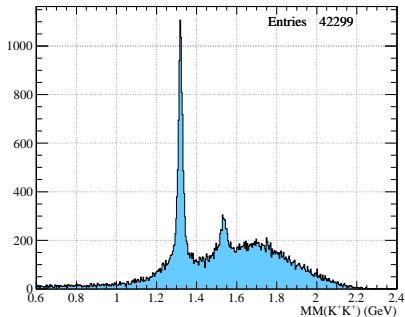
33% of basic cuts

$\Xi^-$  (1530):  $1310 \pm 110$

31% of basic cuts

# Primary Event Selections

$$\gamma p \rightarrow K^+K^+X^-$$



## Event Selections

- Basic Timing Cuts
- TOF Energy Dep.
- Proton

$\Xi^-$  (1320):  $5025 \pm 85$   
22% of basic cuts

$\Xi^-$  (1530):  $1073 \pm 66$   
25% of basic cuts

# Sources of Background

Two types of background sources in  $MM(K^+K^+)$  distribution

## Inefficiencies

- misidentified particles (pions are ID'd as kaons)  
 $\Sigma^{*-}$  states contributed through this and is the largest source of background in this analysis
- wrong beam energy from the tagger

## Competing Physics

- Possibility of many high-mass, broad  $\Xi^{*-}$  states
- $Y^*$  pion emission (soft  $\pi^0$ 's)
- neutral kaon channels such as:
 
$$\gamma p \rightarrow Y^* K^+$$

$$Y^* \rightarrow \Xi^{*0} K^{*0}$$

$$K^{*0} \rightarrow K^+ \pi^-$$

## Part II

# Results From g12







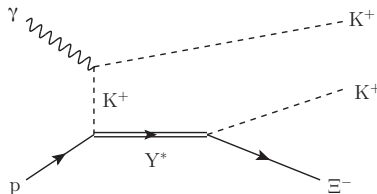




# Model Dependence and Systematic Uncertainty

The model used to simulate Ξ events is the largest source of **systematic** uncertainty.

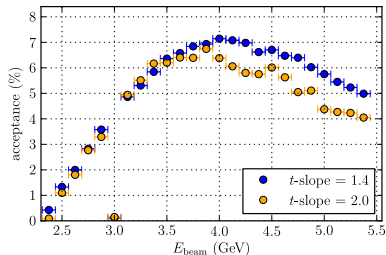
- The model used was a  $t$ -channel production of a  $Y^*$  which then decayed by phase-space to the Ξ
- The major parameters we adjusted to get good agreement with the kaon distributions seen in the data were:
  - $t$ -slope of the leading  $K^+$
  - mass of the  $Y^*$
  - width of the  $Y^*$



# Model Dependence and Systematic Uncertainty

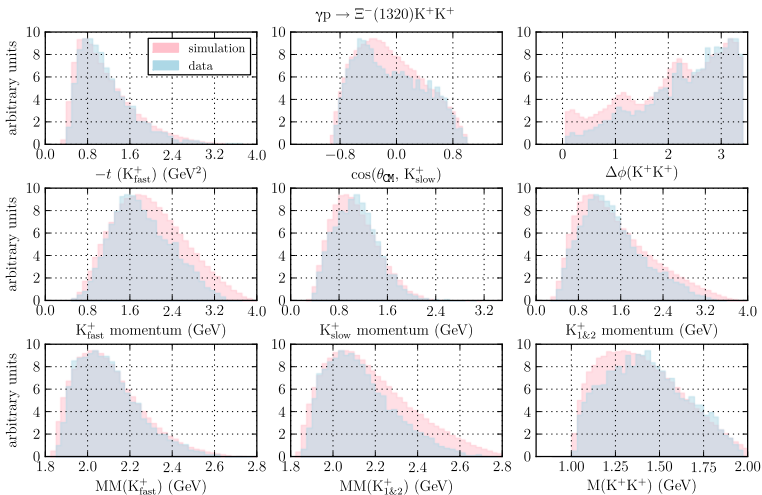
The model used to simulate Ξ events is the largest source of **systematic** uncertainty.

- The model used was a  $t$ -channel production of a  $Y^*$  which then decayed by phase-space to the Ξ
- The major parameters we adjusted to get good agreement with the kaon distributions seen in the data were:
  - $t$ -slope of the leading  $K^+$
  - mass of the  $Y^*$
  - width of the  $Y^*$



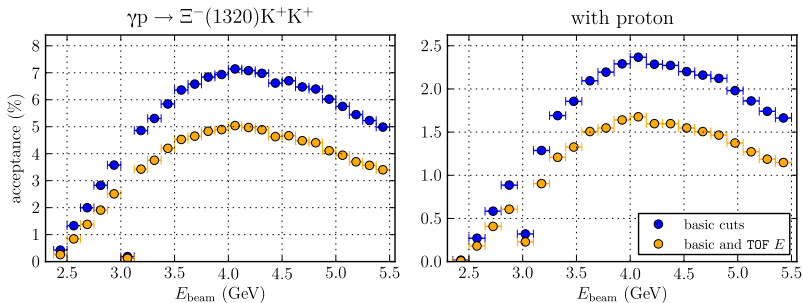
(Similarly for  $Y^*$  mass and width)

# Simulation Comparison to Data



# Acceptance

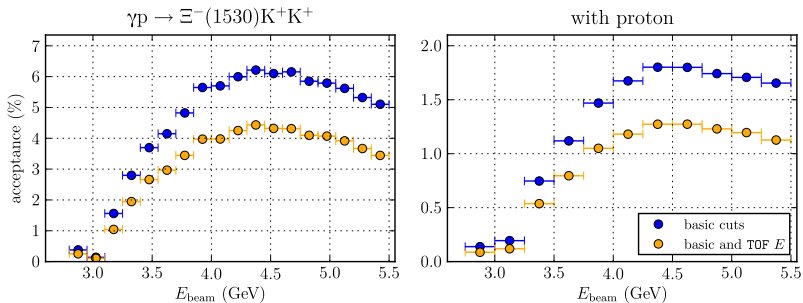
The acceptance for the ground state and first excited  $\Xi^-$  states. The statistical error is within the size of the dots and the systematic error is estimated to be  $\approx 10\%$



$\Xi^-(1320)$

# Acceptance

The acceptance for the ground state and first excited  $\Xi^-$  states. The statistical error is within the size of the dots and the systematic error is estimated to be  $\approx 10\%$



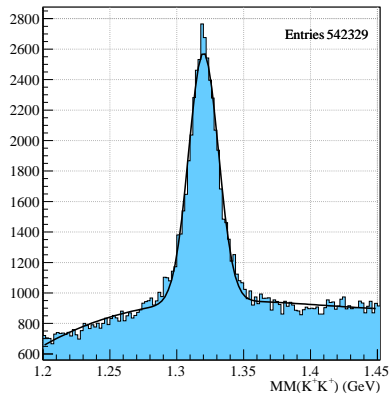
$\Xi^{*-}(1530)$

# Extracting Yields from the Data

- 3<sup>rd</sup> order polynomial
- Gaussian peak
- yield is the integral of the histogram minus the integral of the polynomial part of the total fit.

- There is a systematic uncertainty in this fit
- The shape of the background is not known, but only approximated by the low-order polynomial
- The proton cut gives us a handle on the systematics of this fit indirectly (discussed later)

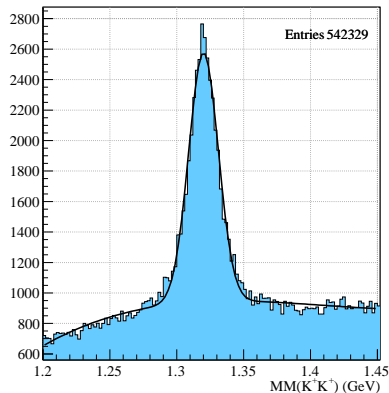
Ξ<sup>-</sup> (1320) fit, full statistics



# Extracting Yields from the Data

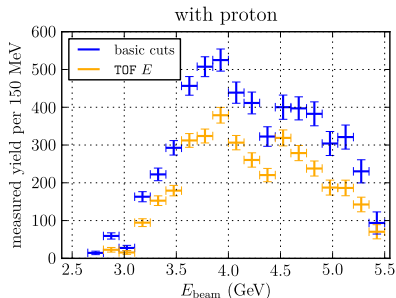
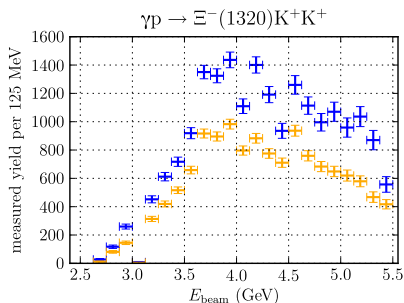
- 3<sup>rd</sup> order polynomial
  - Gaussian peak
  - yield is the integral of the histogram minus the integral of the polynomial part of the total fit.
- 
- There is a systematic uncertainty in this fit
  - The shape of the background is not known, but only approximated by the low-order polynomial
  - The proton cut gives us a handle on the systematics of this fit indirectly (discussed later)

Ξ<sup>-</sup> (1320) fit, full statistics



# Ξ Measured Yields

measured yield of the ground state and first excited state Ξ<sup>-</sup> show structures in acceptance and efficiency of the CLAS detector

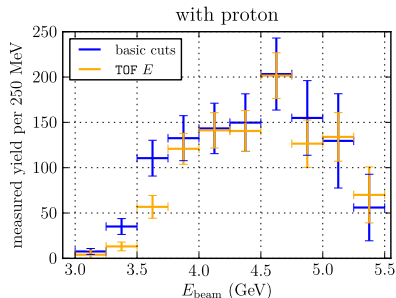
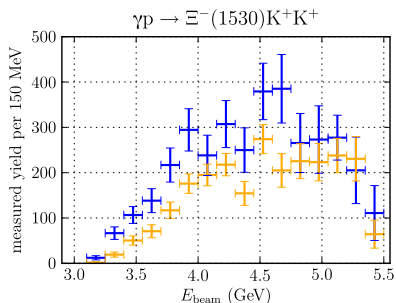


Ξ<sup>-</sup>(1320)

Notice: absence of events at 3 GeV due to bad tagger timing paddle, increases at 3.6 and 4.4 GeV due to trigger configuration

# ≡ Measured Yields

measured yield of the ground state and first excited state  $\Xi^-$  show structures in acceptance and efficiency of the CLAS detector

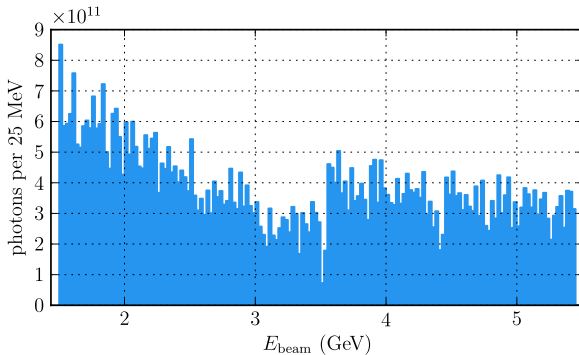


$\Xi^{*-}(1530)$

Notice: absence of events at 3 GeV due to bad tagger timing paddle, increases at 3.6 and 4.4 GeV due to trigger configuration

# Correcting for the Flux

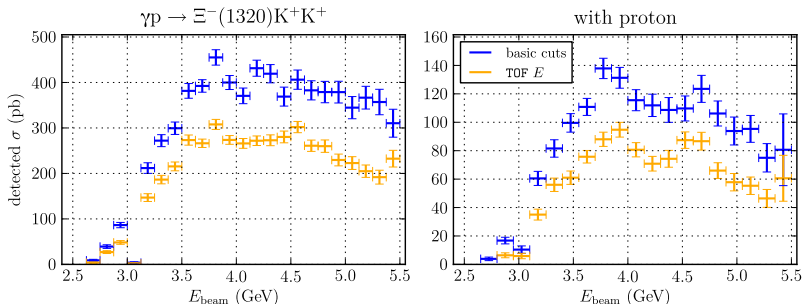
measured yield of the ground state and first excited state  $\Xi^-$  show structures in acceptance and efficiency of the CLAS detector



Photon Flux

# Correcting for the Flux

measured yield of the ground state and first excited state  $\Xi^-$  show structures in acceptance and efficiency of the CLAS detector

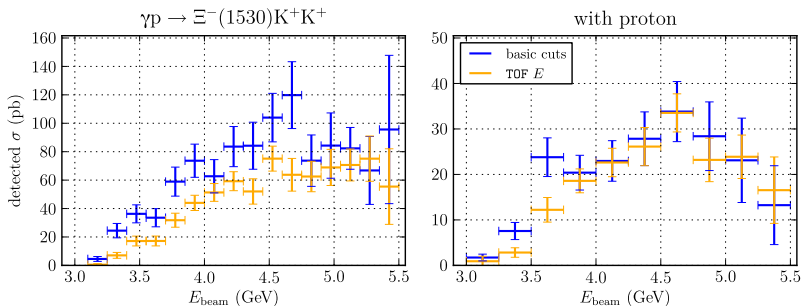


$\Xi^-(1320)$

This includes the target material corrections and is the closest we can get to the final excitation function before we introduce any model

# Correcting for the Flux

measured yield of the ground state and first excited state  $\Xi^-$  show structures in acceptance and efficiency of the CLAS detector



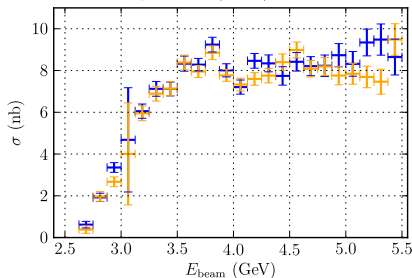
$\Xi^{*-}(1530)$

This includes the target material corrections and is the closest we can get to the final excitation function before we introduce any model

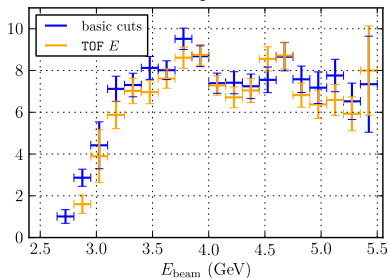
# ≡ Excitation Functions

Total cross section of  $\gamma p \rightarrow \Xi^- K^+ K^+$

$\gamma p \rightarrow \Xi^-(1320) K^+ K^+$



with proton

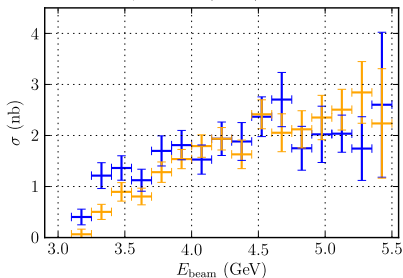


$\Xi^-(1320)$

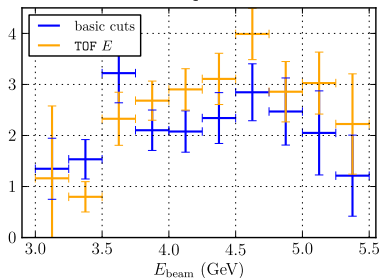
# Ξ Excitation Functions

Total cross section of  $\gamma p \rightarrow \Xi^- K^+ K^+$

$\gamma p \rightarrow \Xi^-(1530) K^+ K^+$



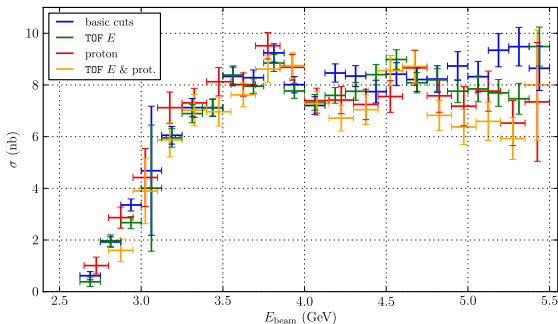
with proton



$\Xi^{*-}(1530)$

# Ξ Excitation Functions

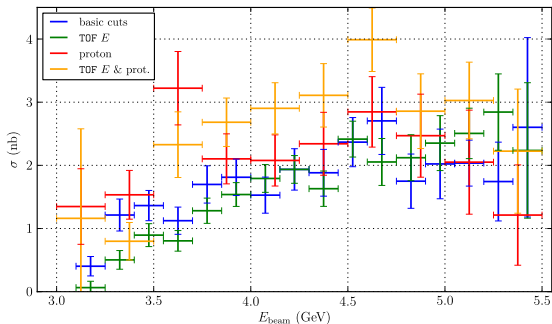
$\gamma p \rightarrow \Xi^- K^+ K^+$   
Total cross section



$\Xi^-(1320)$

# ≡ Excitation Functions

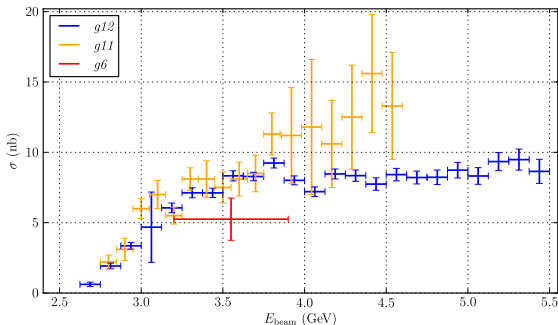
$\gamma p \rightarrow \Xi^- K^+ K^+$   
 Total cross section



$\Xi^{*-}(1530)$

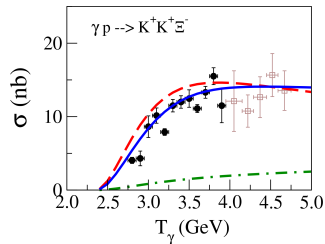
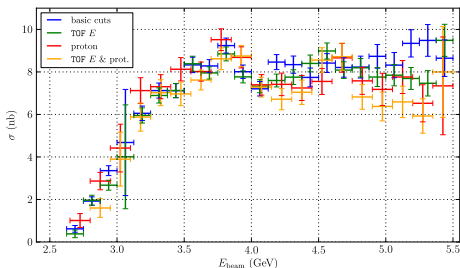
# Comparison to Previous Experiments with CLAS

$\gamma p \rightarrow \Xi^- K^+ K^+$   
Total cross section



# Comparison to Theoretical Work

$\gamma p \rightarrow \Xi^- K^+ K^+$   
 Total cross section



K. Nakayama, Yongseok Oh  
 and H. Haberzettl

Overall scaling factor in prediction was adjusted to g11 data  
 (overlaid points on right)

# Sensitivity of Yield Measurement

- Upper Limit Calculation same as that for Excitation Function ▶ xfn calc
- Differences:
  - Instead of yield, we have the sensitivity to measured yield
  - dependent on the width searched for (25-30 was used for the  $\Xi^*$ )
  - acceptance - similar to  $\Xi(1530)$
  - can't adjust simulation parameters to a signal since there is none!

yield sensitivity was defined as the two standard deviation of the error from the yield measurement which was verified to be consistent with zero



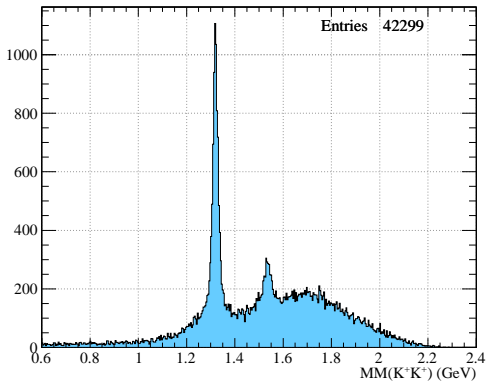






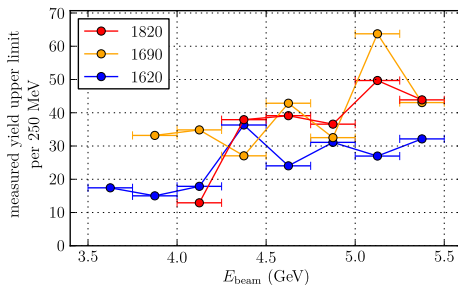
# Missing Mass off $K^+K^+$ Revisited

The proton and the TOF energy deposit cuts were employed in obtaining the upper limits for the  $\Xi^*$  states at 1620, 1690 and 1820 MeV



# $\Xi^*$ Upper Limits

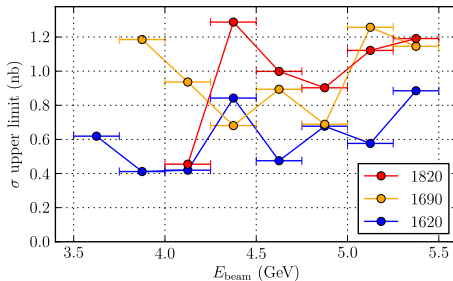
Total cross section upper limits for the  $\Xi^*$  states at:  
1620, 1690 and 1820 MeV



Yield Upper Limits

# $\Xi^*$ Upper Limits

Total cross section upper limits for the  $\Xi^*$  states at:  
1620, 1690 and 1820 MeV



Total Cross Section Upper Limits

## Ξ\* Upper Limits

Total cross section upper limits for the Ξ\* states at:  
1620, 1690 and 1820 MeV

integrated over 3.5–5.4 GeV  
CL = 90%

- Ξ<sup>-</sup>(1620): 0.78 nb
- Ξ<sup>-</sup>(1690): 0.97 nb
- Ξ<sup>-</sup>(1820): 1.09 nb

# Iso-exotic photoproduction

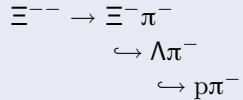
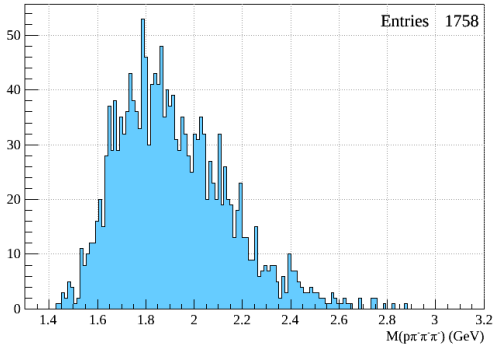
- no reliable model for photoproduction of these states
  - no reliable masses or widths as well
  - qualitative search for narrow resonances
  - depending on the width of these states, the estimated total cross section upper limit are 10–100 nb since statistics are comparable to the search for  $\Xi^{*-}$  data
- 
- only strong decays of the resonances were considered so that definite strangeness could be identified

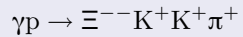
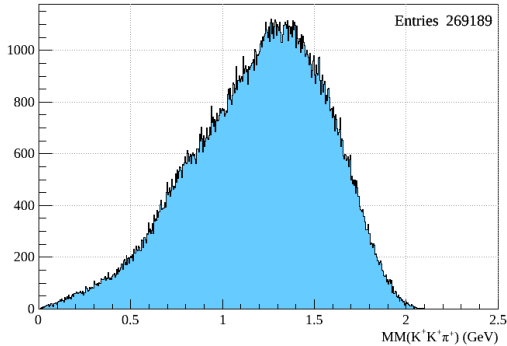
# Iso-exotic photoproduction

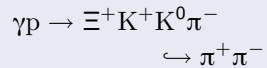
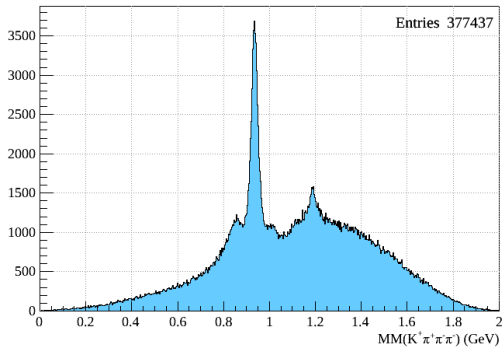
- no reliable model for photoproduction of these states
  - no reliable masses or widths as well
  - qualitative search for narrow resonances
  - depending on the width of these states, the estimated total cross section upper limit are 10–100 nb since statistics are comparable to the search for  $\Xi^{*-}$  data
- 
- only strong decays of the resonances were considered so that definite strangeness could be identified

# Iso-exotic photoproduction

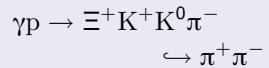
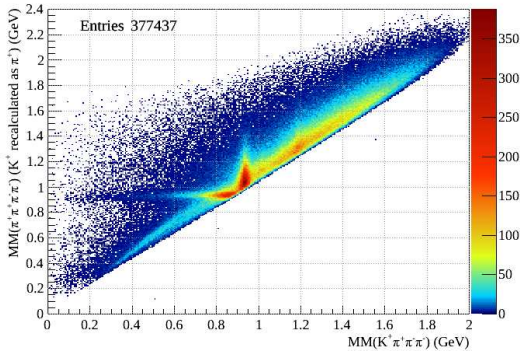
- no reliable model for photoproduction of these states
  - no reliable masses or widths as well
  - qualitative search for narrow resonances
  - depending on the width of these states, the estimated total cross section upper limit are 10–100 nb since statistics are comparable to the search for  $\Xi^{*-}$  data
- 
- only strong decays of the resonances were considered so that definite strangeness could be identified







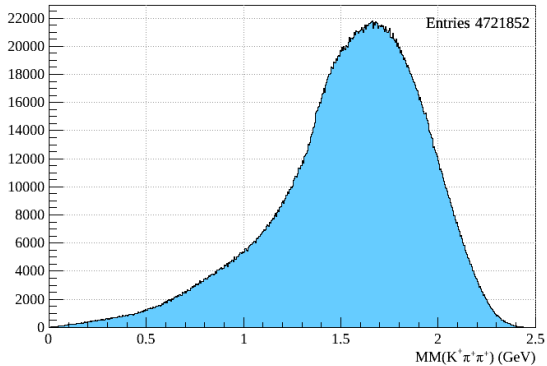
(misidentified pions)



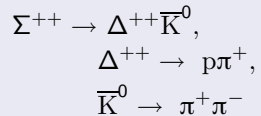
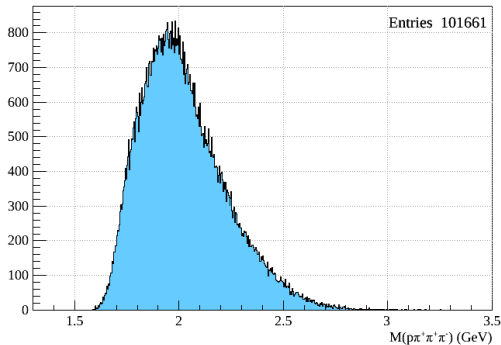
(misidentified pions)



$$\gamma p \rightarrow \Sigma^{--} K^+ \pi^+ \pi^+$$

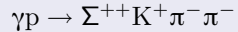
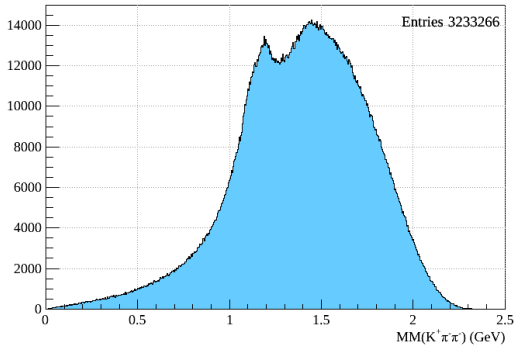


$\Sigma^{++}$



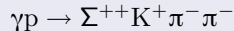
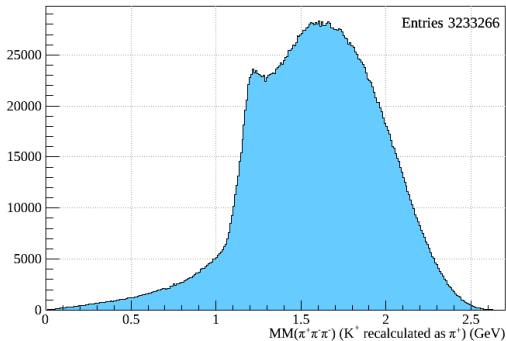
peak at 1232 MeV  
identified as  $\Delta^{++}$  resonance  
(misidentified pions)

$\Sigma^{++}$



peak at 1232 MeV  
identified as  $\Delta^{++}$  resonance  
(misidentified pions)

$\Sigma^{++}$



peak at 1232 MeV  
identified as  $\Delta^{++}$  resonance  
(misidentified pions)

# Summary

- higher mass  $Y^*$ 's contribute to  $\Xi$  production at higher CM energies
- photoproduction total cross sections for the  $\Xi^{*-}$  states above 1530 MeV are smaller than anticipated (no higher than 2 nb)
- This is consistent with the “vector meson dominance” model of the photon (see Fig. 17 on page 20 of dissertation) where the production ratio means we expect 75 events for the  $\Xi^{*-}(1690)$  in g12 — we are only sensitive to about 250 events  
above comparison breaks down due to the difference in beams:  
 $\Sigma^-$  beam vs.  $\gamma$  beam  
but it is the only type of measurement available
- no evidence for iso-exotic baryons of strangeness  $-1$  or  $-2$  (estimated sensitivity  $\approx 10$ – $100$  nb)

# Summary

- higher mass  $Y^*$ 's contribute to  $\Xi$  production at higher CM energies
- photoproduction total cross sections for the  $\Xi^{*-}$  states above 1530 MeV are smaller than anticipated (no higher than 2 nb)
- This is consistent with the “vector meson dominance” model of the photon (see Fig. 17 on page 20 of dissertation) where the production ratio means we expect 75 events for the  $\Xi^{*-}(1690)$  in  $g_{12}$  — we are only sensitive to about 250 events  
above comparison breaks down due to the difference in beams:  
 $\Sigma^-$  beam vs.  $\gamma$  beam  
but it is the only type of measurement available
- no evidence for iso-exotic baryons of strangeness  $-1$  or  $-2$  (estimated sensitivity  $\approx 10$ – $100$  nb)

# Summary

- higher mass  $Y^*$ 's contribute to  $\Xi$  production at higher CM energies
- photoproduction total cross sections for the  $\Xi^{*-}$  states above 1530 MeV are smaller than anticipated (no higher than 2 nb)
- This is consistent with the “vector meson dominance” model of the photon (see Fig. 17 on page 20 of dissertation) where the production ratio means we expect 75 events for the  $\Xi^{*-}(1690)$  in  $g_{12}$  — we are only sensitive to about 250 events

above comparison breaks down due to the difference in beams:

$\Sigma^-$  beam vs.  $\gamma$  beam

but it is the only type of measurement available

- no evidence for iso-exotic baryons of strangeness  $-1$  or  $-2$  (estimated sensitivity  $\approx 10$ – $100$  nb)

# Summary

- higher mass  $Y^*$ 's contribute to  $\Xi$  production at higher CM energies
- photoproduction total cross sections for the  $\Xi^{*-}$  states above 1530 MeV are smaller than anticipated (no higher than 2 nb)
- This is consistent with the “vector meson dominance” model of the photon (see Fig. 17 on page 20 of dissertation) where the production ratio means we expect 75 events for the  $\Xi^{*-}(1690)$  in g12 — we are only sensitive to about 250 events  
above comparison breaks down due to the difference in beams:  
 $\Sigma^-$  beam vs.  $\gamma$  beam  
but it is the only type of measurement available
- no evidence for iso-exotic baryons of strangeness  $-1$  or  $-2$   
(estimated sensitivity  $\approx 10$ – $100$  nb)

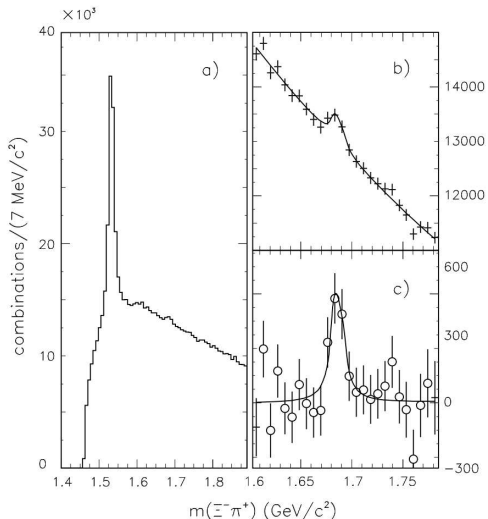
# Summary

- higher mass  $Y^*$ 's contribute to  $\Xi$  production at higher CM energies
- photoproduction total cross sections for the  $\Xi^{*-}$  states above 1530 MeV are smaller than anticipated (no higher than 2 nb)
- This is consistent with the “vector meson dominance” model of the photon (see Fig. 17 on page 20 of dissertation) where the production ratio means we expect 75 events for the  $\Xi^{*-}(1690)$  in  $g_{12}$  — we are only sensitive to about 250 events  
above comparison breaks down due to the difference in beams:  
 $\Sigma^-$  beam vs.  $\gamma$  beam  
but it is the only type of measurement available
- no evidence for iso-exotic baryons of strangeness  $-1$  or  $-2$  (estimated sensitivity  $\approx 10$ – $100$  nb)

## Possible Future Work

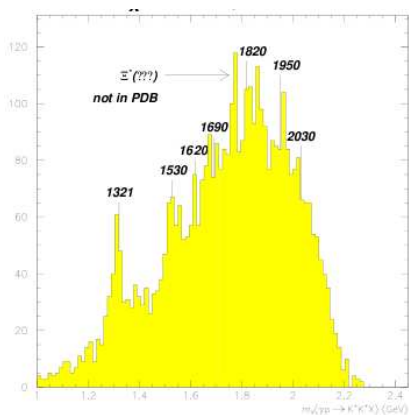
- $\Xi^-$  and  $\Xi^{*-}$  differential cross section measurement  
(requires work on the simulation model used)
- $\Xi^0$  differential and total cross section (neutral kaon channel)
- $\Omega^-$  photoproduction (never seen!)
- mapping out accurate upper limits for the iso-exotics as functions of mass and width

# Ξ(1530) : Ξ(1690) ratio in kaon production



- Invariant mass of  $\Xi^- \pi^+$  using the  $\Sigma^-$  beam at CERN from Adamovich et al., 1997
- this measured ratio equates to  $\geq 75$   $\Xi(1690)$  events in g12 data
- only experimental evidence that a factor of 10 more statistics would be enough to observe the  $\Xi(1690)$

# Keep this plot?



found in  $g12$  proposal (a CLAS internal report)